Energy Economics 111 (2022) 106076

Contents lists available at ScienceDirect

Energy Economics

journal homepage: www.elsevier.com/locate/eneeco

A volatility spillover analysis with realized semi(co)variances in Australian electricity markets

Evelyn Chanatásig-Niza [a], Aitor Ciarreta [b], Ainhoa Zarraga [a,*]

[a] Department of Quantitative Methods, University of the Basque Country UPV/EHU, Avda. Lehendakari Aguirre, 83, 48015 Bilbao, Spain
[b] Department of Economic Analysis, University of the Basque Country UPV/EHU, Avda. Lehendakari Aguirre, 83, 48015 Bilbao, Spain

ARTICLE INFO

JEL classification:
Q41
C32

Keywords:
Electricity prices
Volatility spillovers
Semivariance
Semicovariance
Asymmetric effects

ABSTRACT

Volatility spillovers are a characteristic of interconnected electricity markets. We use high-frequency prices to analyze the transmission of volatility across five Australian regional electricity markets. We propose several models: The first includes only realized variances; the second adds realized covariances; the last two include positive and negative realized semi(co)variances, separately, obtained from the decomposition of the realized covariance matrix into components based on the sign of the underlying returns. We carry out the analysis for both static and dynamic frameworks and relate the behavior of spillovers to major events and policies affecting the markets. Results show that ignoring covariances results in spillovers being underestimated and highlight the importance of the role of semi(co)variances in detecting asymmetric spillovers. Finally, we discuss implications for short-run market participants and long-term planning by regulators.

1. Introduction

In recent years, many countries have moved to deregulate electricity markets to enhance competition. The goal is to make markets more efficient. Market interconnection plays a fundamental role because it is a significant structural characteristic that determines the extent and speed with which shocks spread across markets. Various indexes have been proposed for measuring market interdependence. The very nature of electricity sets it apart from other commodities and financial assets.[1] As a result, volatility risk is a major concern for the efficient operation of interconnected markets.[2] The structural characteristics of markets also play a significant role in price formation.[3] In addition, the deployment of large scale intermittent generation from renewables and increases in the capacity for interconnection between organized markets pose new challenges for market participants. The former is a further source of uncertainty in price formation, and the latter enables volatility shocks to be smoothed over more quickly.

In this context, the analysis of volatility spillovers across electricity markets has become an important issue. An electricity market is likely to be affected by external shocks coming from neighboring connected electricity markets. For volatility shocks to propagate between markets there must be sufficient capacity for interconnection, so the analysis of spillover effects is especially important for market agents to manage portfolios for operating in different electricity markets. In the literature, spillovers are measured in various ways. One approach is to use Markov Regime Switching models, as done by Lindström and Regland (2012) to measure interdependence between six European electricity markets. Another is principal component analysis (see for instance Yan and Trück (2020) for the Australian market). Other authors use multivariate GARCH models to study the level of integration of electricity markets and price convergence, e.g. Worthington et al. (2005) and Higgs (2009) for the Australian, and Ciarreta and Zarraga (2015) for several European markets. Finally, others apply the Diebold and Yilmaz (2009, 2012, 2014) method (hereinafter referred to as DY) based on decomposing forecast error variance using a Vector Autoregressive (VAR) model. This enables various volatility spillover measures to be constructed at different stages, from pairwise directional to overall spillovers, thus providing a more comprehensive analysis than other methods. Examples include Han et al. (2020) and Apergis et al. (2017) for Australian regional markets and Do et al. (2020) for the Irish and British markets.

* Corresponding author.
E-mail addresses: echanatasig001@ikasle.ehu.eus (E. Chanatásig-Niza), aitor.ciarreta@ehu.eus (A. Ciarreta), ainhoa.zarraga@ehu.eus (A. Zarraga).

[1] Electricity prices in worldwide deregulated markets are characterized by mean reversion, seasonality, stationarity, extreme jumps, high volatility, and non-positive and zero prices (see Chan et al. (2008)).

[2] See Ignatieva and Trück (2016) and Apergis et al. (2019) for a discussion on how market risk exposure is associated with these features.

[3] See for instance Wilson (2002) for the role of imperfect competition in market design and Cramton (2017) for the gains from interconnection related to the existence of robust spot markets.

https://doi.org/10.1016/j.eneco.2022.106076
Received 21 April 2021; Received in revised form 6 May 2022; Accepted 9 May 2022
Available online 20 May 2022

Fengler and Gisler (2015) extend the DY approach to include covariances in a multivariate Heterogeneous Autoregressive (HAR) model to analyze spillovers in US financial markets. The inclusion of covariances seeks to measure the joint variability of pairs of market returns. Their use enables the way in which the relationship between two markets affects a third market to be analyzed, which in turn provides a better understanding of the transmission of spillovers. In interconnected markets, the volatility received or transmitted is expected to come from different channels. However, most of the literature on electricity price volatility uses measures of volatility spillovers that ignore the degree of relationship between two markets. Park et al. (2006) and Bunn and Gianfreda (2010) show that the integration of electricity markets could depend not only on geographical proximity or interconnections but also on the maturity and importance of markets. In this context, the use of covariances enables relationships between markets to be described that are not identified using variances alone. Moreover, the sign of the covariance shows the tendency in the linear relationship between pairs of variables. If larger (smaller) returns in one market correspond to the higher (lower) values in another market, then returns tend to show similar behavior. In the opposite case, when greater (smaller) values of one variable mainly correspond to the lower (higher) values of the other, the covariance is negative. Therefore, ignoring covariances means that important channels of volatility spillovers may potentially be missed.

In financial markets, negative (positive) returns are often associated with upward (downward) volatility. This empirical phenomenon is often referred to as asymmetric volatility, and is also observed in electricity prices.[4] Thus, Bollerslev et al. (2020) distinguish between volatility arising from negative return shocks and positive return shocks. In electricity markets Apergis et al. (2017) and Do et al. (2020) measure asymmetries in volatility connectedness coming from good volatility (positive returns) and bad volatility (negative returns). The former find asymmetric spillovers across Australian regional markets, and the latter across the Irish and British markets. However, none of them include covariances in their analyses.

Our contribution is to connect the research line of Fengler and Gisler (2015) with those of Apergis et al. (2017) and Do et al. (2020). The former include covariances in a multivariate HAR model using realized volatility, and the latter analyze asymmetric volatility spillovers across markets. We hypothesize that the use of covariances improves the estimation of volatility spillover measures and provides a better understanding of market interconnections. We also decompose the realized covariance matrix into components based on the sign of the price returns as per Bollerslev et al. (2020) and Bollerslev (2021) and apply the DY (2009, 2012, 2014) approach to analyze volatility spillovers across five interconnected electricity markets in Australia using high-frequency data. Australia is an interesting case study because it is an isolated country that contains several markets with limited levels of interconnection, which implies a larger volatility risk; it is heavily dependent on fossil-fuel generation (especially coal), so it has barriers to effective transition to renewable generation deployment not faced by other liberalized markets. Its markets also differ in size and technology mix.

As far as we know, this approach has not been applied before. We perform a static analysis and a time-varying dynamic analysis. The latter enables us to analyze the dynamics of volatility spillovers across markets and the impact of specific events. The empirical results are expected to be of interest to market participants. A better understanding of the dynamics of volatility spillovers can help to design efficient electricity policies and reduce market risk levels.

The rest of the paper is set out as follows. Section 2 overviews the Australian National Electricity Market. Section 3 presents the data used in the study. Section 4 outlines the econometric methodology used. Section 5 presents the results, and Section 6 discusses some conclusions and recommendations for market participants.

2. Overview of the Australian electricity market

The Australian electricity market comprises two main markets. The first is the Wholesale Electricity Market (WEM), which has been operating since 2006 and supplies electricity to the South-West of Western Australia via the South West Interconnected System. The WEM supplies power to more than one million customers thanks to its 7,800 km of transmission lines. The second is the National Electricity Market (NEM), a wholesale spot market which has been operating since December 1998. It is one of the world's longest interconnected systems. The market owns 40,000 km of transmission lines and cables, and covers a distance of around 5,000 km.[5] The NEM supplies electricity to Queensland (QLD), New South Wales (NSW), Victoria (VIC), Tasmania (TAS), and South Australia (SA). Both markets are operated by the Australian Electricity Market Operator (AEMO), which manages electricity and gas systems and markets across Australia.

The spot market matches supply offers from power stations with real time consumption by households and businesses such that a 5-minute dispatch price is obtained. This represents the cost of supplying the last megawatt of electricity to meet demand, and is applied to all participating generators regardless of the level of their original offer. The dispatch electricity price is important because it is used to determine the spot price for each 30-minute trading interval. It is the average of the last six dispatch prices during the preceding half hour. An increase in the spot price causes generators to increase their energy outputs by turning on their more expensive generators. Conversely, if the spot price is decreasing the more expensive generators are turned down or off.[6] The cost of supply has a price floor of Australian $\$-1,000$ and a maximum price or price cap of $\$14,000$ (Australian Energy Market Commission, AEMC, 2020).

Historically, coal is the main generation source in the NEM. In our sample period (July 2009–February 2019) it accounts on average for more than 70% of total generation. In 2010, the share of renewable electricity generation in Australia was still low: It ranked seventh lowest out of the 28 member countries of the International Energy Agency. According to the Organization for Economic Cooperation and Development (OECD), Australia was one of the highest emitters of greenhouse gases (Australian Energy Regulator, AER, 2012). The country is far from meeting its commitment under the Paris climate agreement. This led the Australian Government to introduce the Carbon Price Mechanism (CPM), a policy focused on cutting carbon and other greenhouse emissions to at least 5% below 2000 levels by 2020 (AER, 2012). The CPM started on 1 July 2012 and ended on 30 June 2014, and it had a limited effect on the generation mix. For example, comparing 2010 with 2019, coal-fired output dropped from 74.6% to 68%, and renewable generation increased from 6.8% to 17.4% of the total generation output (Australian Energy Regulator, AER, 2010, 2020). Carbon generation is larger than the average in OECD countries, which is around 22% (International Energy Agency, IEA, 2020).

By 2019 total generation in the NEM was 198.73 TWh, about 135.14 TWh of which was from coal power plants, with the rest breaking down as follows: Gas 15.98 TWh, wind 14.97 TWh, hydro 14.15 TWh, grid-scale solar 5.82 TWh, rooftop solar 11.82 TWh, and battery energy storage systems 0.07 TWh (Australian Energy Market Operator, AEMO, 2020). QLD, NSW, and VIC are the regions with the biggest coal fired

[4] Knittel and Roberts (2005) and Ciarreta and Zarraga (2016) show evidence of asymmetric responses with a larger effect of positive shocks on volatility. This is known as the inverse leverage effect.

[5] See Table A.1 in Appendix A for existing interconnection capacity for each pair of regions.

[6] There is a contract market for long-term transactions. The contracts reduce retailers' exposure to wide price fluctuations in the spot market, since retailers set fixed prices for longer periods of time.

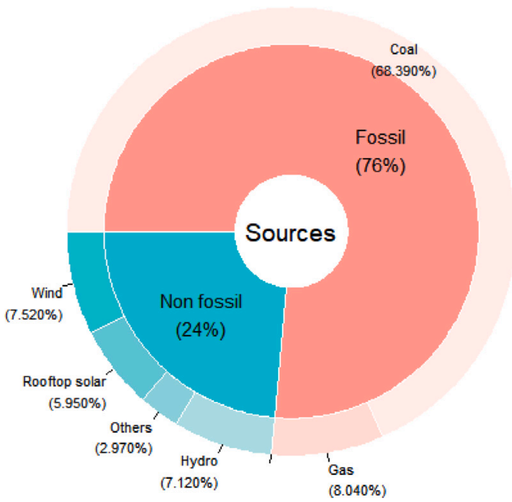

Fig. 1. Percentage of generation accounted for by each source in 2019.
Source: AEMO (2020) and own work.

Table 1
Percentage of generation accounted for per source and demand per state in 2019.
Source: AEMO (2020).

	Sources		Demand
	Fossil	Non fossil	
NSW	81	19	36.6
QLD	87	13	28.7
SA	50	50	6.4
TAS	6	94	5.5
VIC	79	21	22.8

Fossil and Non fossil represent the percentage of each generation source in each state. Demand represents the percentage of total electricity demand per state.

power stations whereas SA relies on gas (48%) and wind generation (38%). TAS is highly dependent on hydro power generation, which accounts for at least 80% of its total. Fig. 1 illustrates the share of each resource in the generation mix for 2019. In addition, Table 1 summarizes the percentage of fossil and non-fossil generation and electricity demand by state in 2019.

Differences in generation capacity, demand size, and technology mix have significant implications for the net selling positions of the regions. NSW, QLD and VIC are the largest markets and the generation mix depends to a large extent on fossil sources. Historically, QLD and VIC have been net exporters of electricity. However, two years after the closure of Hazelwood in April 2017, increases in demand with no further increase in installed capacity made VIC a net importer for the first time. Both NSW and SA have traditionally been net importers. SA and TAS are mainly renewable producers and their net positions as importers or exporters depend heavily on weather conditions (see AER, 2020, and Fig. B.1 in Appendix B).

3. Data

The data-set consists of continuously-recorded 5-minute dispatch electricity prices from 1 July 2009 to 28 February 2019, measured in Australian \$/MWh for five regions: NSW, QLD, SA, TAS, and VIC.[7] Each day thus has 288 trading intervals in each of the five regions under study. Fig. 2 shows the time series of the prices for each market.

[7] Source: https://aemo.com.au/energy-systems/electricity/national-electricity-market-nem/data-nem/market-management-system-mms-data/dispatch

We compute the returns as $r_{ji} = P_{ji} - P_{ji-1}$, where P_{ji} represents the original electricity price for the jth market in the ith interval of time. The presence of zero and negative prices prevents logarithms in prices from being taken. Following Andersen et al. (2001) and Bollerslev et al. (2020) we estimate the realized daily variation and covariation using the covariance matrix definition, so:

$$ReCov = \sum_{i=1}^{m} r_i r_i' = \begin{bmatrix} ReVar_{NSW} & ReCov_{NSW-QLD} & \cdots & ReCov_{NSW-VIC} \\ ReCov_{QLD-NSW} & ReVar_{QLD} & \cdots & ReCov_{QLD-VIC} \\ \vdots & \vdots & \ddots & \vdots \\ ReCov_{VIC-NSW} & ReCov_{VIC-QLD} & \cdots & ReVar_{VIC} \end{bmatrix} \tag{1}$$

where $r_i = (r_{NSW,i}, r_{QLD,i}, r_{SA,i}, r_{TAS,i}, r_{VIC,i})'$ for $i = 1, \dots, m$, with m being the number of returns in a day.[8] Eq. (1) represents the covariance matrix made up of the realized variance of each market on the diagonal and the realized covariances across the markets on the off-diagonal.

The realized measures capture the real volatility in the markets but cannot identify what fractions of the total variation come from positive and negative returns. Barndorff-Nielsen et al. (2010) decompose the realized variance into two estimators which capture the variation due to positive and negative movements. The downside (or negative) realized semivariances focus on squared negative returns while the upside (or positive) realized semivariances focus on squared positive returns. In recent papers, Bollerslev et al. (2020) and Bollerslev (2021) propose the decomposition of the realized covariance matrix into realized semicovariances dictated by the sign of the underlying high frequency returns.

Define r_i^+ and r_i^- as the positive and negative returns, respectively. "Concordant" realized semicovariance matrices associated with the realized covariance matrix are:

$$\begin{aligned} \hat{P} &= \sum_{i=1}^{m} r_i^+ (r_i^+)', \\ \hat{N} &= \sum_{i=1}^{m} r_i^- (r_i^-)' \end{aligned} \tag{2}$$

The concordant matrices $\hat{P}$ and $\hat{N}$ comprise the positive and negative realized semivariances on their diagonals, and the positive and negative realized semicovariances on the off-diagonals. "Discordant" semicovariance matrices are defined as:

$$\hat{M} = \underbrace{\sum_{i=1}^{m} r_i^+ (r_i^-)'}_{\hat{M}^+} + \underbrace{\sum_{i=1}^{m} r_i^- (r_i^+)'}_{\hat{M}^-} \tag{3}$$

where $\hat{M}^+$ and $\hat{M}^-$ have zeros on their diagonals and the scalar realized semicovariances obtained from opposite-signed returns on the off-diagonals. Note that for any sampling frequency m, $ReCov = \hat{P} + \hat{N} + \hat{M}^+ + \hat{M}^-$.

To obtain series with normal distribution, which is required for the generalized variance decomposition (see Section 4.2), a variance stabilizer is applied to the realized measures. We use the transformation in Uniejewski et al. (2017), which is based on the so-called probability integral transform (PIT): $Z_t = G^{-1}(\hat{F}(X_t))$, where X_t is the realized measure to be transformed, $\hat{F}$ is the distributional forecast of the cumulative distribution function (cdf) of X_t, and G^{-1} is the inverse of the standard normal cdf.

[8] Note that this is a continuous market, so we only miss the first return in the whole sample.

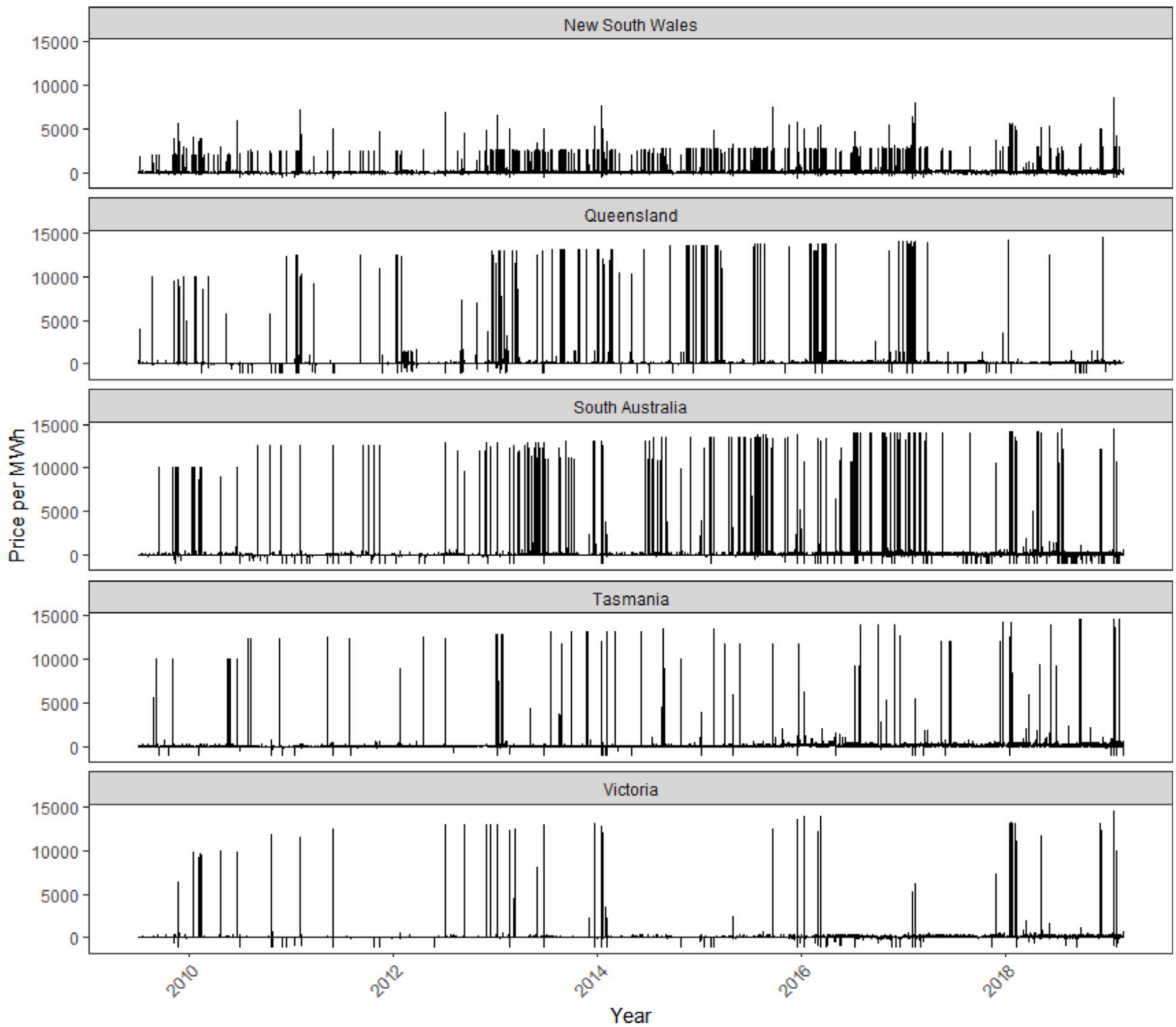

Fig. 2. Intraday dispatch electricity prices in five Australian markets.

4. Methodology

4.1. The multivariate HAR model

Corsi (2009) proposes a Heterogeneous Autoregressive (HAR) model, which is an AR-type model with the difference that it considers realized volatility over different time horizons, which enables it to describe heterogeneity from markets. Based on Corsi (2009), we propose the following models:

- MHAR-ReVar: Multivariate HAR model using realized variances.
- MHAR-ReCov: Multivariate HAR model using realized variances and covariances.
- MHAR-ReCov$^+$: Multivariate HAR model using positive realized semi(co)variances.
- MHAR-ReCov$^-$: Multivariate HAR model using negative realized semi(co)variances.

The models suffer from a high-dimensional parameter space. To deal with this issue we estimate them using the Least Absolute Shrinkage and Selection Operator (LASSO) proposed by Tibshirani (1996). Audrino and Knaus (2016) suggest that LASSO performs favorably when the data generator process is the HAR model.

4.1.1. The MHAR-ReVar model

We specify the model as:

$$Y_t = \beta_0 + \sum_{h\in\{1,7,30\}} \beta_h Y_{h,t-1} + \epsilon_t \tag{4}$$

where Y_t denotes a column vector formed by the N realized variances ($N = 5$ markets), β_0 is an $N \times 1$ vector containing the intercepts, β_h is an $N \times N$ coefficient matrix, ϵ_t is an $N \times 1$ vector of zero mean and finite variance innovations, and $Y_{h,t-1}$ is the h-period average of the past realized variances:

$$Y_{h,t-1} = \frac{1}{h}\sum_{i=1}^{h} Y_{t-i}$$

The choice of h corresponds to one day ($h = 1$), one week ($h = 7$), and one month ($h = 30$). Introducing different horizons means that three primary volatility components can be described: short-term, medium-term, and long-term. The importance of including them is that volatility over longer time intervals has a stronger influence on shorter time intervals than conversely (Corsi, 2009).

4.1.2. The MHAR-ReCov model

To analyze the role of covariances in the transmission mechanism, we consider an unrestricted model which takes into account realized variances and covariances as in Fengler and Gisler (2015). Assuming that markets are interconnected through common information flows, including covariances in the models reduces the loss of spillover information. We specify the model as:

$$\tilde{Y}_t = \tilde{\beta}_0 + \sum_{h\in\{1,7,30\}} \tilde{\beta}_h \tilde{Y}_{h,t-1} + \tilde{\epsilon}_t \quad (5)$$

where $\tilde{Y}_t = vech(ReCov)$ is the K-dimensional, half-vectorized time-t daily realized covariance matrix of size N, i.e. $K = N(N+1)/2$, estimated using the high-frequency data of N electricity markets.[9] $\tilde{\beta}_0$ is a vector containing K intercepts, $\tilde{\beta}_h$ are $K \times K$ coefficient matrices, $\tilde{Y}_{h,t-1}$ contains the three volatility components corresponding to time horizons of one day, one week, and one month, and $\tilde{\epsilon}_t$ is a $K \times 1$ vector of zero mean and finite variance innovations.

4.1.3. The MHAR-ReCov$^+$ and MHAR-ReCov$^-$ models

Following Bollerslev et al. (2020) and Bollerslev (2021), we specify the MHAR-ReCov model allowing for positive and negative semi(co) variances separately, taking advantage of the information given by the signs of the returns.

$$Y^*_t = \beta^*_0 + \sum_{h\in\{1,7,30\}} \beta^*_h Y^*_{h,t-1} + \epsilon^*_t \quad (6)$$

For the MHAR-ReCov$^+$ model, Y^*_t is a K dimensional vector which contains the positive realized semi(co)variances of each element belonging to the lower triangular realized covariance matrix, which are calculated using $\hat{P}$ and $\hat{M}^+$ from Eqs. (2) and (3), β^*_0 is a $K \times 1$ vector of intercepts, β^*_h is a $K \times K$ coefficient matrix, $Y^*_{h,t-1}$ contains positive semi(co)variances estimated in Eqs. (2) and (3) corresponding to time horizons of one day, one week, and one month, and ϵ^*_t is a $K \times 1$ vector of zero mean and finite variance innovations. Analogously, the MHAR-ReCov$^-$ model contains the negative realized semi(co)variances calculated using $\hat{N}$ and $\hat{M}^-$ from Eqs. (2) and (3).

As Fengler and Gisler (2015) show, the multivariate HAR models proposed are constrained VAR(30) models in which the DY (2009, 2012) methodology, explained below, can be applied.

4.2. Volatility spillover measures

DY (2009, 2012) propose estimating volatility spillovers using the forecast error variance decomposition from a vector autoregressive model (VAR) using the Generalized Variance Decomposition (GVD) proposed by Koop et al. (1996) and Pesaran and Shin (1998). DY (2009, 2012) consider a covariance stationary VAR(p) model:

$$Y_t = \sum_{i=1}^{p} \phi_i Y_{t-i} + \epsilon_t,$$

where Y_t represents the vector of dependent variables in Eqs. (4), (5) and (6), ϕ_i represents a coefficient matrix, and $\epsilon \sim (0, \Sigma)$ is a vector of independently and identically distributed disturbances. The moving average representation of the VAR is:

$$Y_t = \sum_{i=0}^{\infty} A_i \epsilon_{t-i}$$

where A_i represents a matrix obtained by the recursion $A_i = \phi_1 A_{i-1} + \phi_2 A_{i-2} + \dots + \phi_p A_{i-p}$ with A_0 being the identity matrix and $A_i = 0$ for $i < 0$.

The variance decomposition identifies the percentage of the H-step-ahead error variance in forecasting Y_i associated with shocks to Y_j for $j \neq i$. As DY (2012) explain, this requires orthogonal innovations which can be calculated using Cholesky factorization or the method in Koop et al. (1996) and Pesaran and Shin (1998). We employ the latter approach because it has the advantage of producing variance decomposition invariant to the ordering of the variables. For a forecast horizon H, the decomposition of the error variance into the variance components attributable to the different variables is given by:

$$\theta^g_{ij}(H) = \frac{\sigma^{-1}_{jj} \sum_{h=0}^{H-1} (e'_i A_h \Sigma e_j)^2}{\sum_{h=0}^{H-1} (e'_i A_h \Sigma A'_h e_i)},$$

where g refers to the GVD method, σ_{jj} is the variance of the error term for the jth equation, and e_i is the binary selection vector, with one as the ith element and zero otherwise. DY (2012) propose normalizing each entry in the variance decomposition matrix so that the sum of contributions to the forecast error variance is one. The fraction of the H-step-ahead forecast-error variance of Y_i due to exogenous shocks to Y_j is given by:

$$\widetilde{\theta}^g_{ij}(H) = \frac{\theta^g_{ij}(H)}{\sum_{j=1}^{N} \theta^g_{ij}(H)}$$

We estimate an aggregate index, the total volatility spillover index (TSI), which measures the contribution of volatility spillover shocks across variables to the total forecast error variance:

$$S^g(H) = \frac{\sum_{i,j=1,i\neq j}^{N} \widetilde{\theta}^g_{ij}(H)}{\sum_{i,j=1}^{N} \widetilde{\theta}^g_{ij}(H)} \cdot 100 = \frac{\sum_{i,j=1,i\neq j}^{N} \widetilde{\theta}^g_{ij}(H)}{N} \cdot 100$$

The TSI also makes it possible to identify the directional spillovers, which are estimated using the normalized elements of the generalized decomposition matrix. The spillovers transmitted by market i to all other markets j are defined as:

$$S^g_{.i}(H) = \frac{\sum_{\substack{j=1\\ j\neq i}}^{N} \widetilde{\theta}^g_{ji}(H)}{N} \cdot 100$$

Analogously, the spillovers received by market i from all markets j are measured by:

$$S^g_{i.}(H) = \frac{\sum_{\substack{j=1\\ j\neq i}}^{N} \widetilde{\theta}^g_{ij}(H)}{N} \cdot 100$$

DY (2012) define the net directional spillovers from market i to all markets j as the difference between the volatility spillovers transmitted to and those received from the rest of the markets:

$$S^g_i(H) = S^g_{.i}(H) - S^g_{i.}(H)$$

Additionally, the use of semi(co)variances in the estimation of model (6) enables a distinction to be drawn between spillovers coming from positive and negative returns and therefore it is possible to quantify the asymmetries in the volatility spillovers over time.

Following Baruník et al. (2015) we compute the spillover asymmetry measure (SAM) as:

$$SAM = S^+ - S^-$$

where S^+ and S^- are volatility spillover measures due to positive and negative semi(co)variances, i.e. obtained from MHAR-ReCov$^+$ and MHAR-ReCov$^-$ models, respectively. A positive SAM indicates that spillovers from positive realized semi(co)variances are larger than those from negative realized semi(co)variances, and the opposite is true for a negative SAM. By contrast, if SAM takes a value of zero the volatility spillover measures are symmetric.

5. Results

This section presents the empirical findings on volatility spillovers in the Australian NEM. The results are divided into two subsections: Static analysis and dynamic analysis. The former enables the volatility spillovers to be analyzed using the full sample. The latter enables the time-varying dynamics of volatility spillovers to be analyzed using a rolling window of 365 days.

[9] $vech(.)$ corresponds to the lower triangular elements of the realized covariance matrix. Note that with five markets in the system ($N = 5$), there is a 15×1 column vector (five variance equations and 10 covariance equations).

DY (2014) explain that as the forecast horizon lengthens there may be more chances for connectedness to appear. However, in electricity markets short-term fluctuations are important because price level and volatility can change from one day to another and within a day, despite seasonal fluctuations. We therefore select one-day-ahead as our forecast horizon. This is also the horizon used by AEMO for pre-dispatch forecasts.

5.1. Static analysis

We estimate models (4), (5), and (6) using LASSO for the full sample. Tables 2, 3, and 4 summarize the volatility spillover results. The ijth entry in each table represents the contribution to the forecast-error variance of the realized (co)variance i from innovations to the realized (co)variance j. All tables show both the direction and the size of the spillovers in the market[10]. "Directional TO others" measures the spillovers from each market to the rest and is obtained as the sum of the elements of the column corresponding to each market excluding the current one. "Directional FROM others" measures the spillovers to each market from the rest and is obtained as the sum of the elements of the row corresponding to each market excluding the current one. The last row contains the net volatility spillovers and the value of the TSI. The net directional spillovers identify whether a state is a contributor to or recipient of volatility. A negative value indicates that the spillovers transmitted by the market are lower than those received, while a positive value indicates the opposite.

Table 2 reports the variance spillovers estimated with the MHAR-ReVar. The TSI is 47.40%, so approximately 47% of the forecast error variance for the entire market comes from spillover effects, while the rest is due to internal shocks in the regional markets. This result is close to that obtained by Han et al. (2020) in the NEM for 2010–2017 and highlights that most of the volatility of the markets is explained by their own shocks.

Regarding directional spillovers, NSW is the largest transmitter and receiver ($S^g_{.NSW}$ = 77.28% and $S^g_{NSW.}$ = 59.89%) of spillovers. This result is expected since NSW is the biggest market and its degree of interconnection with VIC (one interconnector) and QLD (two interconnectors) is one of the largest. NSW also has the largest generation capacity in the market, and is a historical net importer in the NEM (see Table A.1 in Appendix A). As expected, lower spillover effects are observed between those regions which are not physically interconnected. The pairwise spillovers from QLD to SA and from QLD to TAS are the lowest (2.76% and 1.82%), and those from SA to QLD and from TAS to QLD (3.57% and 1.91%) are also low. Finally, NSW and VIC are both net-contributors, while QLD, SA, and TAS are net-recipients. Our findings indicate that overall QLD, SA, and TAS are affected by fluctuations in NSW and VIC.

Table 3 shows the spillovers estimated from the MHAR-ReCov model. The TSI indicates that approximately 68% of the volatility forecast error variance comes from spillovers. This value is larger than that of the MHAR-ReVar model, which evidences that excluding covariances from the volatility measures means losing a channel of information in the NEM and therefore underestimating the spillovers. Covariances permit an explanation to be found as to how volatility in market i can affect the relationships between other markets. For example, agents in market i could import electricity to cover demand or to obtain a financial benefit by exporting to other regions where prices are higher. This last behavior can be explained with the use of covariances.

Pairwise directional spillovers provide a better understanding of the connection between electricity markets. As expected, the highest spillovers are the diagonal elements which represent the share of own (co)variances. As regards off-diagonal elements, the highest pairwise directional spillovers are those for the variance of QLD and the covariance QLD-NSW (23.40% and 22.66%, respectively). In this case, the price volatility in QLD is highly affected by the strong link between the QLD and NSW markets. We attribute this result to technical conditions between the two markets such as close alignment of prices and a fairly stable duration of network congestion.

There are also high pairwise directional spillovers between the variance of SA and SA-NSW covariance (20.46% and 22.23%, respectively). Although these markets are not physically connected, the results suggest a strong link between them. Park et al. (2006) mention that the maturity and importance of one market could affect others which are physically further away. In the case of SA-NSW covariance we argue that the fact that they are historical importers leads the two regions to share similar patterns.

High pairwise directional spillovers are also observed between the VIC-NSW and VIC-SA covariances (14.53% and 17.45%). Both regions are interconnected with VIC and import electricity from it. It could therefore be inferred that price volatility between VIC-NSW is affected by the VIC-SA covariance. From an economic perspective this makes sense because generators would prefer to sell their surpluses in the region that offers the higher price as long as transmission between the regions is possible.

Other noteworthy directional spillovers are those between the covariances VIC-TAS and TAS-SA (15.40% and 15.88%). This result suggests that the price variation between TAS and SA is affected by the covariance between VIC and TAS. In this case, VIC plays the role of a transit state between SA and TAS so at certain times of the day it can profit from that position. Thus, traders find opportunities for arbitrage between these two markets.

By contrast, the lowest pairwise directional spillovers, though they are still significant, are those for the variance of TAS and the covariance SA-QLD, and for the variance of TAS and the covariance QLD-NSW (all below 1%). QLD can be considered a peripheral state which is fully connected only to NSW. Its relationships with other geographically distant markets are thus less important, which explains the results.

Various features also stand out in Table 3. For the "Directional TO others" row the biggest spillover transmitters are found to be the covariance VIC-NSW (98.43%) and the variances of VIC and NSW (96.89% and 87.91%). This is not surprising because VIC and NSW are the most connected regions in the NEM. This result is similar to that obtained by Han et al. (2020), who explain that factors such as consumption, the level of interconnections, and the capacity for the generation and exporting of electricity to other markets in NEM enable VIC be the biggest transmitter. This result contrasts with that obtained for the MHAR-ReVar model, where VIC is the second-biggest spillover transmitter (56.95%) behind NSW (77.28%). The reason for this difference is that the MHAR-ReCov model takes into account the linkage between the markets through covariances, which further explain the transmission of spillovers. These results remain when the "Directional FROM others" column is analyzed. The covariance VIC-NSW and the variances of VIC and NSW receive the largest spillovers.

Just as important but of smaller size are the directional spillovers that the variance of NSW and the covariance SA-NSW receive ($S^g_{NSW.}$ = 74.30% and $S^g_{SA-NSW.}$ = 73.14%) and those that they transmit ($S^g_{.NSW}$ = 87.91% and $S^g_{.SA-NSW}$ = 81.00%). The smallest directional spillovers are those of the covariances TAS-QLD, and SA-QLD, and the variance of TAS, so they are the least significant spillover receivers but also the least significant spillover transmitters. This is expected since TAS has the lowest interconnection capacity and is thus unable to transmit or receive much volatility to or from the other markets. In the case of TAS-QLD and SA-QLD covariances, geographical distance and lack of interconnections explain the results.

Analysis of the "NET Directional" row shows that the results for the variances are similar to those obtained in Table 2. For the full sample

[10] We test the significance of all the spillover measures using bootstrapped standard errors with 1000 resamplings calculated following the approach in Lütkepohl (2000) for VAR models.

Table 2
Spillovers based on MHAR-ReVar for the full sample period.

	NSW	QLD	SA	TAS	VIC	Directional FROM others
NSW	40.11	18.75	18.40	8.85	13.88	59.89
QLD	26.42	58.87	3.57	1.91	9.24	41.13
SA	21.50	2.76	49.45	4.16	22.13	50.55
TAS	14.29	1.82	6.37	65.83	11.70	34.17
VIC	15.07	6.63	21.91	7.66	48.73	51.27
Directional TO others	77.28	29.96	50.25	22.57	56.95	237.01
NET Directional	17.39	−11.17	−0.30	−11.60	5.68	**TSI=47.40**

The table shows spillovers for the full sample for a forecast horizon of 1 day based on the MHAR-ReVar model. The ij entry of the upper-left 5 × 5 submatrix estimates the fraction of one-day-ahead error variance in forecasting market i due to exogenous shocks to market j. The "Directional FROM others" and "Directional TO others" figures represent the directional spillovers, and "NET Directional" represents the net directional spillovers. Bootstrapped standard errors with 1000 resamplings are used to test the significance of the spillover measures. All the measures are statistically significant at the 1% level.

Table 3
Spillovers based on MHAR-ReCov for the full sample.

	NSW	QLD	SA	TAS	VIC	QLD - NSW	SA - NSW	TAS - NSW	VIC - NSW	SA - QLD	TAS - QLD	VIC - QLD	TAS - SA	VIC - SA	VIC - TAS	Directional FROM others
NSW	25.70	11.92	11.67	5.61	8.60	7.78	10.48	3.07	4.09	1.55	0.92	1.82	1.24	2.99	2.56	74.30
QLD	15.49	34.36	2.05	1.14	5.21	22.66	2.34	0.85	3.66	2.63	1.29	3.35	1.13	2.46	1.38	65.64
SA	13.20	1.64	30.16	2.53	13.38	0.81	22.23	1.13	4.26	1.07	0.64	1.21	0.99	3.53	3.24	69.84
TAS	8.14	1.05	3.56	37.28	6.60	0.59	3.24	21.71	3.94	0.48	1.23	0.76	3.47	3.08	4.87	62.72
VIC	7.62	3.26	11.08	3.93	24.87	2.09	9.30	2.78	11.36	2.03	1.02	2.86	3.27	9.41	5.13	75.13
QLD-NSW	10.27	23.40	0.97	0.58	3.27	33.51	1.51	0.83	4.17	7.26	2.73	5.43	1.78	3.09	1.19	66.49
SA-NSW	10.97	1.73	20.46	2.18	10.28	1.12	26.86	1.70	6.88	3.38	1.87	3.11	1.57	3.82	4.08	73.14
TAS-NSW	3.90	0.67	1.37	19.42	4.05	0.75	2.10	31.81	6.76	1.67	4.57	1.83	9.50	5.19	6.43	68.19
VIC-NSW	3.80	2.42	3.74	2.45	11.79	2.83	6.37	4.90	23.66	3.62	2.27	6.99	6.11	14.53	4.54	76.34
SA-QLD	2.25	2.93	1.33	0.49	3.19	8.59	5.03	2.01	6.04	38.74	5.82	17.59	1.55	3.57	0.87	61.26
TAS-QLD	1.60	1.79	0.88	1.38	2.10	3.68	2.92	6.35	4.27	6.24	42.51	8.61	6.74	1.74	9.19	57.49
VIC-QLD	2.46	3.44	1.46	0.70	4.42	5.57	4.20	2.12	10.72	15.27	7.25	34.68	1.44	4.53	1.74	65.32
TAS-SA	1.71	1.04	1.22	3.41	4.98	1.72	2.04	10.14	8.69	1.32	5.16	1.16	32.60	8.93	15.88	67.40
VIC-SA	3.28	1.97	3.71	2.34	11.76	2.61	4.35	4.48	17.45	2.75	1.18	3.54	7.57	28.41	4.60	71.59
VIC-TAS	3.23	1.27	3.60	4.36	7.27	1.10	4.89	6.69	6.15	0.70	6.81	1.39	15.40	5.01	32.13	67.87
Directional TO others	87.91	58.52	67.10	50.51	96.89	61.90	81.00	68.77	98.43	49.96	42.75	59.65	61.75	71.86	65.70	1022.70
NET Directional	13.62	−7.11	−2.74	−12.21	21.75	−4.58	7.86	0.58	22.09	−11.29	−14.73	−5.67	−5.65	0.27	−2.17	**TSI= 68.18**

The table shows spillovers for the full sample for a forecast horizon of 1 day based on the MHAR-ReCov model. The ij entry of the upper-left 15 × 15 submatrix estimates the fraction of one-day-ahead error variance in forecasting market i due to exogenous shocks to market j. The "Directional FROM others" and "Directional TO others" figures represent the directional spillovers, and "NET Directional" represents the net directional spillovers. Bootstrapped standard errors with 1000 resamplings are used to test the significance of the spillover measures. All the measures are statistically significant at the 1% level.

Table 4
Spillovers based on MHAR-ReCov^{+} and MHAR-ReCov^{-} for the full sample.

	NSW	QLD	SA	TAS	VIC	QLD - NSW	SA - NSW	TAS - NSW	VIC - NSW	SA - QLD	TAS - QLD	VIC - QLD	TAS - SA	VIC - SA	VIC - TAS	Directional FROM others
Panel A: Spillovers based on MHAR-ReCov^{+}																
NSW	26.08	12.01	11.83	5.66	8.63	8.45	9.81	3.16	4.17	0.81	0.82	1.29	1.46	3.37	2.45	73.92
QLD	15.69	35.23	2.01	1.17	5.31	23.86	1.91	0.73	3.31	2.23	1.06	2.59	0.99	2.54	1.37	64.77
SA	13.06	1.58	30.10	2.46	13.10	1.08	21.88	1.23	4.84	0.58	0.51	1.22	1.19	4.08	3.09	69.90
TAS	8.14	1.07	3.54	37.26	6.46	0.57	2.90	22.32	4.02	0.42	1.52	0.71	3.76	3.21	4.10	62.74
VIC	7.56	3.28	11.02	3.86	24.96	2.29	9.17	2.69	12.07	1.66	0.93	2.87	3.04	9.83	4.78	75.04
QLD-NSW	11.59	25.42	1.33	0.55	3.63	35.35	1.65	0.54	3.48	5.44	1.93	4.28	1.12	2.36	1.34	64.65
SA-NSW	10.35	1.36	20.96	1.97	10.37	1.16	27.84	1.61	7.83	2.38	1.13	3.15	1.54	4.36	3.99	72.16
TAS-NSW	4.30	0.66	1.69	20.48	4.29	0.52	2.11	32.32	6.35	1.00	5.53	1.88	9.09	4.61	5.19	67.68
VIC-NSW	3.91	2.18	4.40	2.51	12.71	2.27	7.14	4.49	24.05	2.61	2.08	7.30	4.89	14.77	4.69	75.95
SA-QLD	1.37	2.91	0.90	0.57	3.25	6.95	4.08	1.54	5.35	44.77	5.59	18.51	0.95	2.28	0.99	55.23
TAS-QLD	1.62	1.64	0.79	1.91	2.01	2.62	1.94	8.04	4.25	5.53	44.20	8.49	8.06	1.96	6.93	55.80
VIC-QLD	1.88	2.81	1.61	0.75	4.63	4.21	4.36	2.34	11.56	14.50	7.04	36.34	1.39	4.67	1.91	63.66
TAS-SA	2.21	1.05	1.63	3.92	5.15	1.14	2.12	10.50	7.59	0.61	6.26	1.16	35.88	8.52	12.23	64.12
VIC-SA	3.75	2.08	4.42	2.46	12.44	1.98	4.83	3.99	17.79	1.35	1.22	3.54	6.81	28.61	4.73	71.39
VIC-TAS	3.37	1.43	3.87	3.92	7.41	1.31	5.16	5.75	6.92	0.80	5.21	1.62	11.78	5.50	35.96	64.04
Directional TO Others	88.80	59.45	69.99	52.21	99.40	58.41	79.05	68.94	99.55	39.92	40.83	58.61	56.06	72.07	57.78	1001.05
NET Directional	14.89	−5.32	0.08	−10.53	24.35	−6.25	6.89	1.26	23.60	−15.31	−14.97	−5.05	−8.06	0.67	−6.26	**TSI = 66.74**
Panel B: Spillovers based on MHAR-ReCov^{-}																
NSW	24.95	11.45	11.32	5.46	8.36	8.21	10.79	3.29	4.30	2.23	0.84	2.16	1.37	2.61	2.66	75.05
QLD	15.10	33.94	2.01	1.11	5.24	22.91	2.32	1.05	3.90	2.70	1.26	3.64	1.29	2.25	1.29	66.06
SA	13.07	1.64	29.97	2.56	13.47	0.87	22.34	1.12	4.01	1.69	0.63	1.27	1.16	3.10	3.10	70.03
TAS	8.03	1.03	3.57	36.92	6.62	0.76	3.66	21.58	4.23	0.72	0.85	0.92	3.09	3.01	5.01	63.08
VIC	7.56	3.31	11.22	3.98	24.88	2.19	9.54	2.73	11.06	2.66	0.94	2.96	3.37	8.73	4.86	75.12
QLD-NSW	11.15	24.07	1.09	0.77	3.52	33.88	1.54	1.48	4.24	5.44	2.06	4.87	1.93	2.85	1.11	66.12
SA-NSW	11.37	1.74	20.22	2.41	10.27	1.16	26.18	2.05	6.19	4.62	1.74	3.15	1.58	3.51	3.82	73.82
TAS-NSW	4.25	0.82	1.43	19.39	3.96	1.30	2.66	31.58	6.67	1.83	3.70	1.95	8.81	5.54	6.12	68.42
VIC-NSW	4.20	2.66	3.64	2.71	11.75	2.92	5.94	4.97	24.07	3.94	2.00	7.38	5.19	14.39	4.25	75.93
SA-QLD	3.39	3.10	2.24	0.60	4.09	6.21	6.96	2.12	6.15	37.84	5.84	16.16	1.47	2.82	1.01	62.16
TAS-QLD	1.53	1.77	0.86	1.09	1.94	2.93	2.84	5.61	3.96	6.99	45.00	9.23	7.27	1.90	7.09	55.00
VIC-QLD	3.00	3.76	1.65	0.75	4.56	4.92	4.31	2.21	11.06	14.33	7.03	35.02	1.34	4.19	1.89	64.98
TAS-SA	1.90	1.20	1.44	3.24	5.31	1.96	2.20	10.15	7.71	1.54	5.45	1.18	34.65	9.98	12.09	65.35
VIC-SA	3.06	1.88	3.40	2.45	11.29	2.43	4.10	5.10	17.58	2.46	1.17	3.37	8.16	29.34	4.21	70.66
VIC-TAS	3.67	1.22	3.80	4.97	7.58	1.11	5.12	6.96	6.29	1.02	5.35	1.76	11.90	5.12	34.13	65.87
Directional TO others	91.28	59.61	67.88	51.47	97.96	59.86	84.31	70.41	97.35	52.17	38.88	60.00	57.93	70.01	58.51	1017.66
NET Directional	16.24	−6.44	−2.15	−11.61	22.84	−6.26	10.50	1.99	21.42	−9.99	−16.12	−4.98	−7.43	−0.65	−7.35	**TSI = 67.84**

The table shows spillovers for the full sample for a forecast horizon of 1 day based on the MHAR-ReCov model. The ij entry of the upper-left 15 × 15 submatrix in each panel estimates the fraction of one-day-ahead error variance in forecasting market i due to exogenous shocks to market j. The "Directional FROM others" and "Directional TO others" figures represent the directional spillovers, and "NET Directional" represents the net directional spillovers. Bootstrapped standard errors with 1000 resamplings are used to test the significance of the spillover measures. All the measures are statistically significant at the 1% level.

period NSW and VIC are net-contributors (13.62% and 21.75%) while the remaining markets are net-recipients. In the case of covariances the net-contributors to the volatility in the NEM are formed by four pairs of covariances: VIC-NSW, SA-NSW, TAS-NSW and VIC-SA. It is clearly dominated by the VIC-NSW pairwise positive contribution as it involves the two largest markets.

Table 5
Spillover contributions for the full sample.

	MHAR-ReCov	MHAR-ReCov$^+$	MHAR-ReCov$^-$
Cross variance spillovers	21.83%	23.22%	22.81%
Cross covariance spillovers	20.53%	20.87%	20.95%
Own variance spillovers	13.46%	13.73%	13.38%
Own covariance spillovers	44.18%	42.18%	42.87%

The table shows the spillover contributions to the TSI from variances and covariances based on the MHAR-ReCov, MHAR-ReCov$^+$, and MHAR-ReCov$^-$ models for the full sample.

Table 4 shows the spillover measures based on MHAR-ReCov$^+$ and MHAR-ReCov$^-$ models (panels A and B, respectively). The measures are similar in size to those from the MHAR-ReCov model ignoring the sign of the returns. However, in general, larger spillovers are observed for negative semi(co)variances. Specifically, for TSI 66.74% of the forecast error variance for the entire market is due to spillover effects when only positive semi(co)variances are considered while the figure is 67.84% when only negative semi(co)variances are considered. These figures evidence the presence of asymmetric spillovers.

Following Fengler and Gisler (2015), Table 5 reports own variance spillovers (defined as the spillovers from variances to variances), cross covariance spillovers (defined as the spillovers from covariances to variances), and own covariance and cross variance spillovers, defined analogously, for the MHAR-ReCov, MHAR-ReCov$^+$, and MHAR-ReCov$^-$ models.

The largest contribution to TSI comes from own covariance spillovers; more than 40% of the TSI is explained by the spillovers from covariances to covariances. By contrast, only around 13% is explained by own variance spillovers. This underscores the importance of including covariances in the model and also reveals features of strong interdependence in the NEM. Finally, cross variance and cross covariance spillovers contribute approximately 20% each to TSI. Asymmetric behavior is also observed. Cross and own variance spillovers are larger for positive realized measures while cross and own covariance spillovers are larger for negative realized measures.

To summarize, the results suggest that there is interdependence between the markets which is better described when semi(co)variances are included. Covariances enable a better description to be obtained of the role of interconnection between VIC and VIC-NSW, which can be considered the core of the NEM. Additionally, findings suggest that including covariances improves TSI estimation. For the NEM, Han et al. (2020) report a TSI close to 35% using realized measures and Apergis et al. (2017) a figure of 52% using realized variances. In our analysis the TSI is 68.18% when semi(co)variances are included.

5.2. Dynamic spillover analysis

We estimate models (4), (5), and (6) using a 365-day rolling window, allowing the spillovers to change over time. This dynamic analysis enables the expected impact of different events to be analyzed, such as coal plant closures, high demand in the market, extreme weather conditions, and technical failures (see Table C.1 in Appendix C), plus that of regulation policies on spillovers across markets.

5.2.1. Total spillover index

Fig. 3 shows the time-varying TSI for the MHAR-ReVar and MHAR-ReCov models. It does not remain constant over time and takes values that deviate from those obtained for each model using the full sample. The lowest figure in the TSI series is for the MHAR-ReVar model, whose values range between 37% and 56%. By contrast, the TSI values range between 56% and 77% for the MHAR-ReCov, which shows that most of the total forecast error variance is explained by spillovers. This is in line with the result obtained in the static analysis and highlights that ignoring covariances leads to the TSI being underestimated. Therefore, we continue the comparative analysis with the models that include covariances.

Overall, the TSI has a seasonal component. It shows an upward trend during the summer months, when there are unusual increases in demand associated with higher temperatures. Nationwide extreme weather conditions tend to increase the TSI. This is accentuated by the fact that heat-waves have increased in number and duration (Trancoso et al., 2020). Examples are January–February 2011, when the AER reports days with higher demand than forecast in VIC, NSW and QLD, and a blackout in QLD, which produced higher spillovers in the NEM (see Table C.1 in Appendix C for more details); late December 2012 to early January 2013, when the whole country experienced a heat-wave; and widespread heat-waves in January 2019. There are also market conditions such as congestions and shutdowns that affect volatility transmissions (see Table C.1 in Appendix C).

We find that the TSI does not behave significantly differently during the CPM period than during the periods immediately before and after it. Han et al. (2020) and Apergis et al. (2017) find that the TSI was generally lower and more stable during the carbon pricing period than during the periods before and after. The introduction of the CPM and some external factors such as outages and a decrease in generation led to an increase in the TSI until October 2012. Prices remained high during the CPM period, so volatility spillovers decreased. In summer 2013–2014 prices rose due to high temperatures, which pushed up demand and volatility spillovers. The end of the CPM did not lead to an immediate reduction in prices. Indeed, it took between two and six months for wholesale prices to fall, which led to a steady reduction in volatility spillovers at the end of 2014 (Australian Energy Regulator, AER, 2014). However, there are some mild upward movements mainly due to a number of closures of coal plants from August to November 2014 in VIC and NSW with a loss of more than 1300 MW.

It should be noted that there is a decrease in volatility spillovers from 2016 with the exception of some upward movements due to certain events reported by AER. Specifically, in May 2016 two coal plants were closed in SA, resulting in an increase in prices in the NEM and thus to upward movements in the TSI. In September and December 2016 the entire system suffered failures, which affected principally SA. The biggest occurred in the Heywood Interconnector.[11] The failure caused AEMO to suspend the market in SA and applied administered pricing arrangements from 28 September to 11 October (Australian Energy Regulator, AER, 2017). The closure of Hazelwood power station in April 2017 with a drop of 20% in generation capacity in VIC is also reflected in higher volatility spillovers. Apergis et al. (2017) find that the spillover index in the NEM in 2010–2016 is lower than in 2002–2010 and argue that this could be due to the implementation of the CPM together with the planned transition to an emissions trading scheme (ETS), which could make markets less competitive. They also expect a lower degree of connectedness when the ETS is in full operation. There have also been investments in transmission which have helped to reduce transmission congestion (Brinsmead et al., 2014). These factors explain the steady decline in the TSI observed from 2016 onwards.

[11] In 2016 Heywood was the NEM's most congested interconnector, partly because an upgrade periodically limited its capacity.

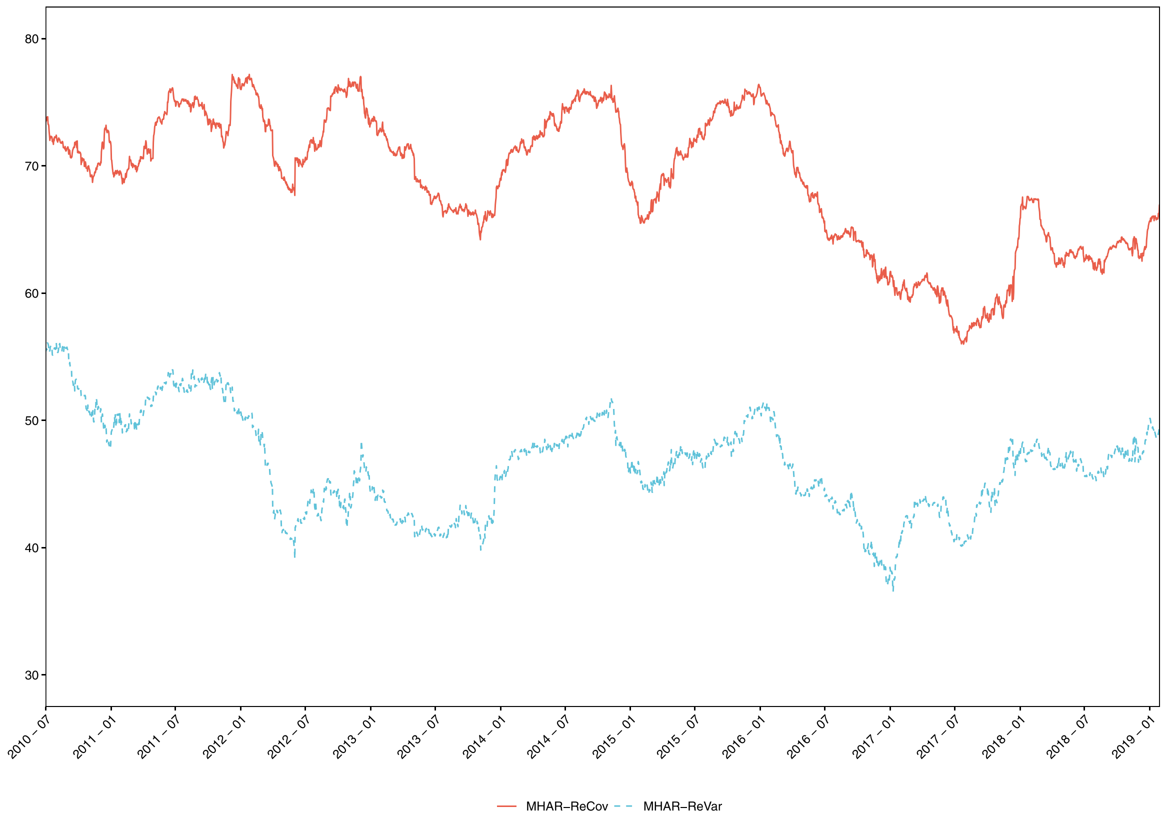

Fig. 3. Time-varying TSI based on MHAR-ReVar and MHAR-ReCov models.

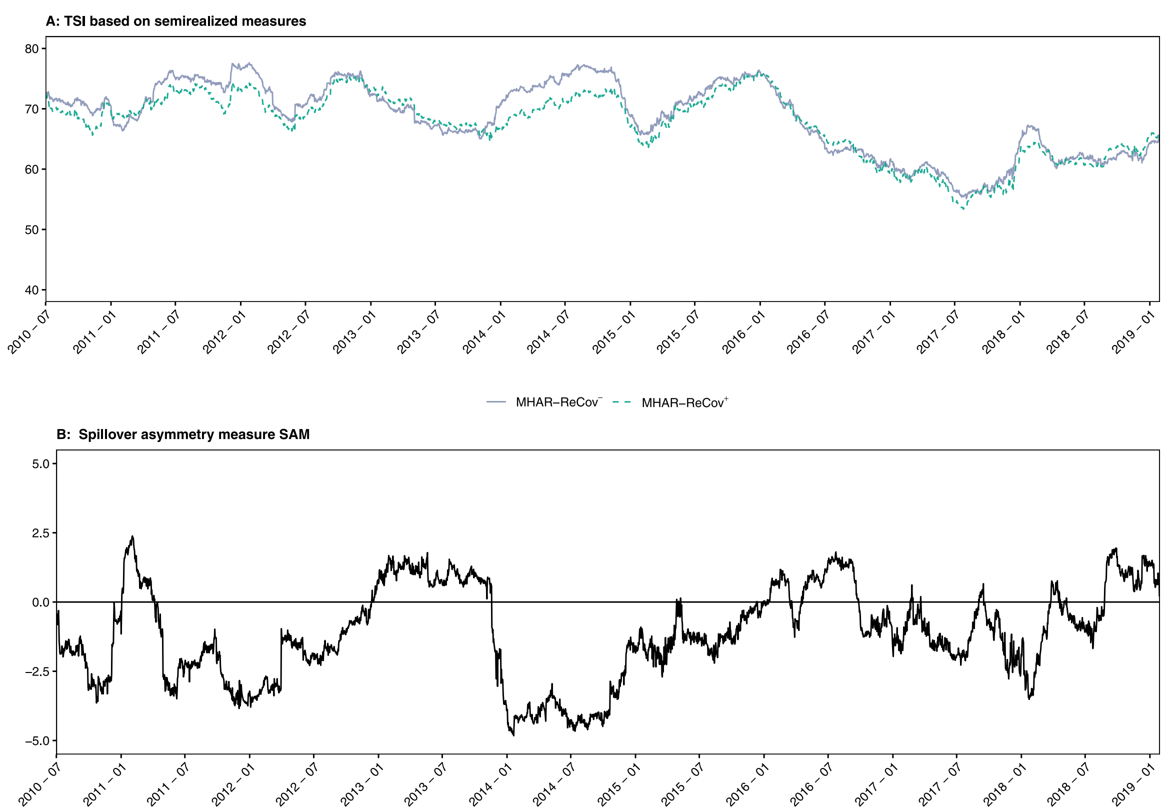

Fig. 4. Time-varying TSI based on MHAR-ReCov$^+$ and MHAR-ReCov$^-$ models.

Fig. 4 shows the time-varying total volatility spillover indexes derived from positive and negative realized semi(co)variances separately (Panel A), and the corresponding time-varying SAM (Panel B). The figure enables the time-varying role of spillovers from different signed returns to be analyzed, and how they could have been affected by events in the NEM during the sample period. Although both TSI series display a similar pattern, spillovers from negative realized semi(co)variances are in general larger than those from positive ones. Specifically, the TSI ranges from 53% to 76% for the MHAR-ReCov$^+$ model and from 55% to 78% for the MHAR-ReCov$^-$ model. The beginning of the sample period is marked by the dominance of spillovers from negative returns, as a result of the presence of negative prices and decrease in demand. Nonetheless, after the entry of the CPM this dominance started to decrease and spillovers from positive returns became the main drivers by the end of 2012 and for most of 2013. As mentioned, the introduction of this carbon tax policy led to an overall increase in prices due to the shutdown of large-scale coal power plants (in NSW and VIC) and deployment of intermittent renewable generation (in SA) with no change in the capacity for interconnection (Australian Energy Regulator, AER, 2013). However in 2014, while the CPM was still in force, negative volatility drivers dominated positive ones, because price spikes became less frequent and volatility due to renewable generation increased (Australian Energy Regulator, AER, 2014). For much of 2016, spillovers in the NEM were driven by positive returns. The closure of various coal plants in SA could explain the increase in prices in this period. From 2017 onwards, negative spillovers are larger than positive ones, though they are smaller.

5.2.2. Directional spillovers

Fig. 5 shows the spillover transmissions "from" and "to", as well as net spillovers for variances in the MHAR-ReCov model. Panel A shows the spillovers "from" and "to" for each region distinguishing the contributions of variances and covariances. In general, the contribution of variances is more stable and smaller than that of covariances for all regions except TAS where the pattern of variance contribution changes noticeably over time. We also observe that the pattern of spillovers is determined by the covariance contribution, which is more volatile. In the case of NSW, the contribution from variance and covariance to spillovers is similar. We relate this result to the characteristics of NSW, such as demand size (see Table 1) and its interconnection capacity (see Table A.1 in Appendix A). By contrast, the spillovers associated with VIC show a larger contribution from covariances. This highlights the fact that VIC is the most interconnected region. In the case of TAS the contribution of variance shows two downward movements. The first is related to the entry into force of the CPM. Although TAS increased its exports it did not have much effect on prices in neighboring regions. The second valley reflects the outage in the Basslink interconnector, which put the cable out of operation for almost six months.

Panel B of Fig. 5 shows the region's net position over time. VIC and NSW are the biggest transmitters and recipients of spillovers in the NEM, which was expected as these are the two largest and most interconnected markets. Moreover, both states are net-transmitters throughout the sample period, as in the static analysis. By contrast, QLD, SA and TAS are mostly net-recipients.

Fig. D.1 in Appendix D shows the spillover transmissions "from" and "to", as well as net spillovers for the covariances in the MHAR-ReCov model. The most important spillovers transmitted "to" others come mostly from VIC-NSW, VIC-SA, SA-NSW, and QLD-NSW. In the case of VIC-NSW and VIC-SA covariances the transmission of spillovers affects other covariances. As mentioned in the static analysis, NSW and SA are net importers of electricity from VIC. Thus, the link described by the covariances between these three markets is expected to remain steady and strong over time.

The volatility in QLD-NSW covariance is observed to affect mainly variances. This is consistent with the findings of the static analysis, where it is evident that $ReVar_{QLD}$ is affected by this covariance. This is because QLD is the largest exporter to NSW.

The time-varying spillovers based on the MHAR-ReCov$^+$ and MHAR-ReCov$^-$ models share a similar pattern to those obtained from the MHAR-ReCov model (see Fig. 6 for variances, and Fig. D.2 in Appendix D for covariances). Therefore, results decomposing covariance

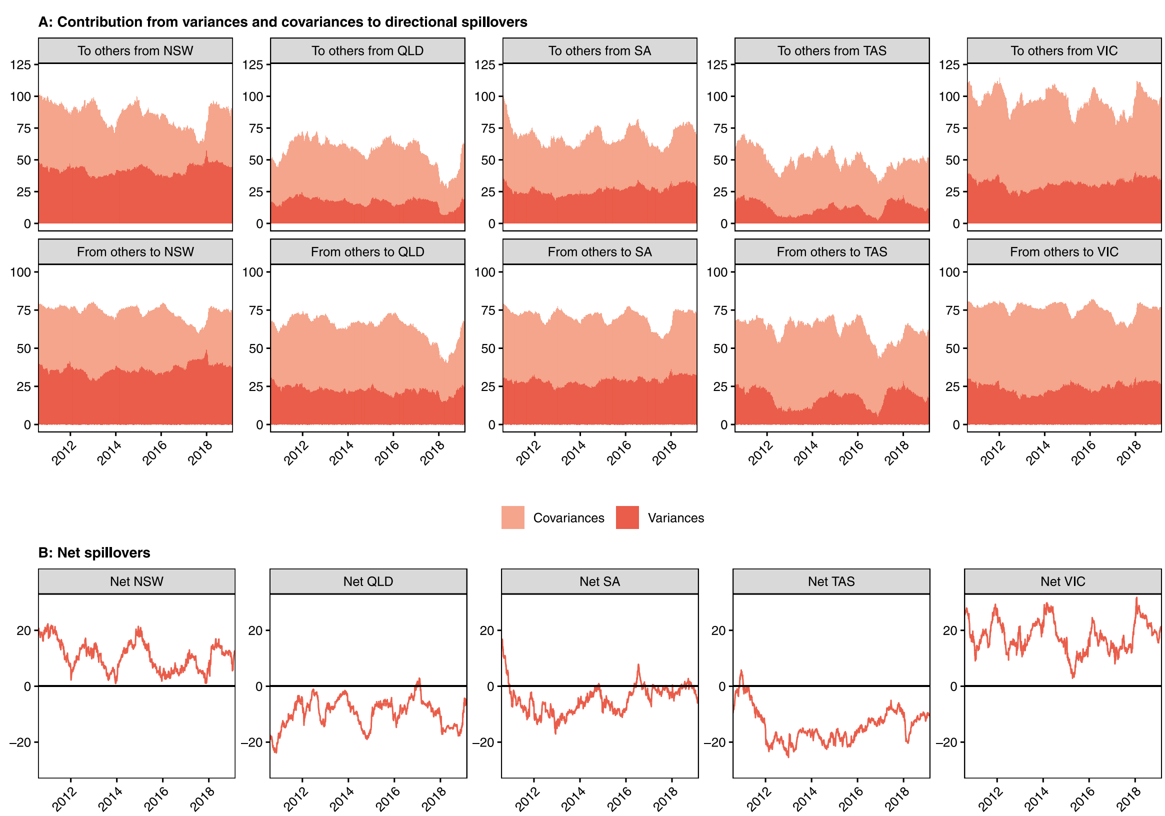

Fig. 5. Time-varying spillovers based on MHAR-ReCov.
Note: Panel A shows the contribution of variances (dark orange) and covariances (light orange) to the directional spillovers. Panel B shows the net directional spillovers. (For interpretation of the references to color in this figure legend, the reader is referred to the web version of this article.)

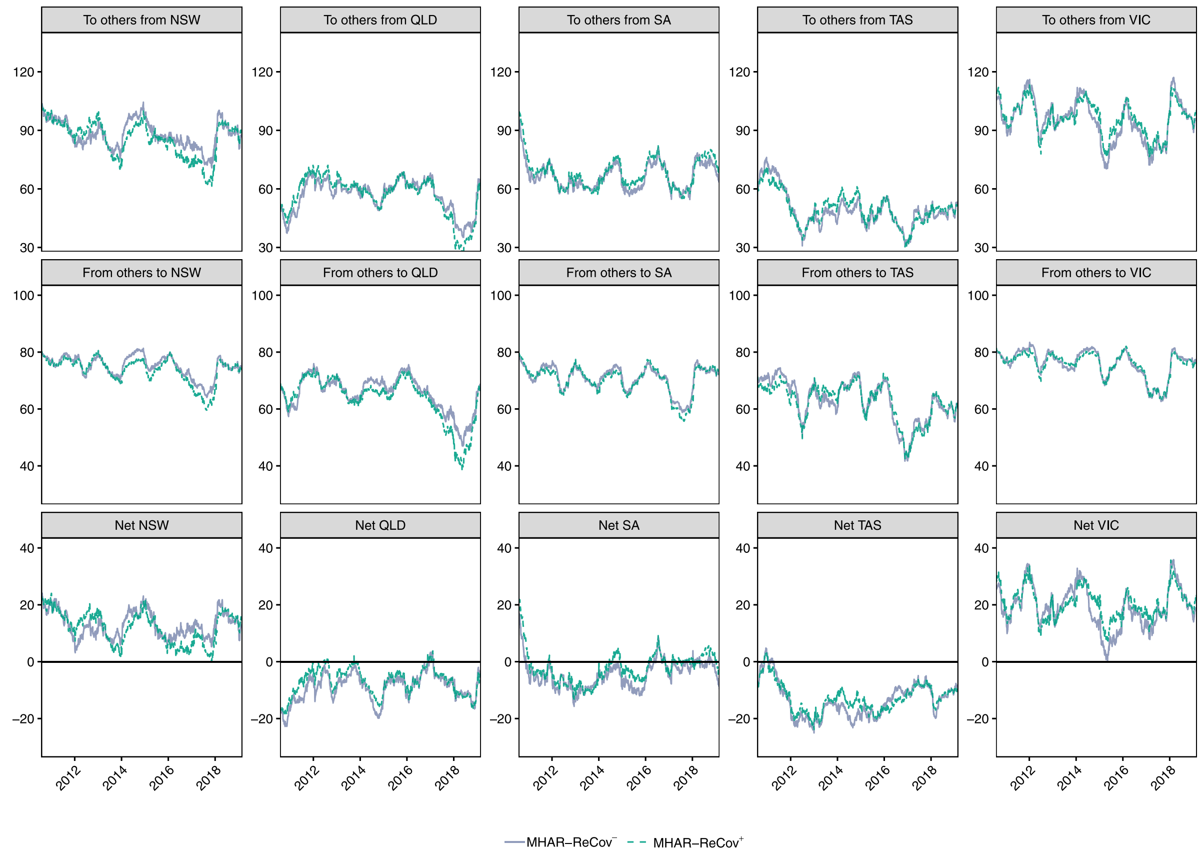

Fig. 6. Time-varying spillovers based on MHAR-ReCov$^+$ and MHAR-ReCov$^-$.

according to the sign of the returns reinforce the role of VIC and NSW as the main transmitters of volatility in the NEM. Nonetheless, some asymmetric spillovers are observed, depending on the region and the direction of transmissions. In general, increases in demand and coal plant closures reported by AER are followed by increases in prices, so that spillovers from positive returns dominate those from negative returns. Analogously, when prices decrease the dominant spillovers are those from negative returns.

5.3. Summary of results

To summarize, the results of the static and dynamic analyses shed light on several issues. It is shown that covariances cannot be ignored in the analysis of spillovers. The largest covariances are related to directly connected markets, but there are other equally important covariances that reveal relationships between non-connected markets. To improve market integration, covariances enable regions with potential opportunities for interconnection investment to be identified.

Our results suggest a strong link between NSW and SA, which backs Project Energy Connect (Australian Energy Regulator, AER, 2020) to build a new interconnector between the power grids of SA and NSW and add a connection between VIC and SA in addition to the existing Heywood and Murraylink. The construction of a new interconnector could provide lower power prices, improve energy security, and increase economic activity between these regions.

Finally, the significance of the sign of the underlying returns cannot be disregarded. The average spillovers in the entire market are in general larger for negative than for positive returns, which indicates that price drops provoke more volatility in the entire market. This indicates that hedging is advisable for businesses to protect against energy price volatility, especially that which comes from negative returns.

6. Conclusions

This study analyzes the pattern of volatility spillovers across five regional markets in the Australian NEM using 5-minute prices for a sample period from 1 July 2009 to 28 February 2019. It investigates the role of covariances and the presence of asymmetries in the transmission mechanism of volatility spillovers. To that end, we decompose the realized covariance matrix following Bollerslev et al. (2020), then estimate the spillover indexes originally proposed by DY (2009, 2012). Finally, we propose several models which are estimated in a comparative static and dynamic analysis.

Results show that including covariances in the model raises the TSI, which shows their importance in explaining volatility spillovers across markets. Most of the volatility observed in each market is explained by external factors that have greater effects on neighboring markets more than on their own. Moreover, the effect of positive and negative shocks analyzed separately is different, which indicates that there are asymmetries in volatility spillovers.

The results of the static and dynamic analyses are along the same lines, but the latter identifies episodes of volatility spillovers throughout the sample period which can be related to market structural changes, weather conditions and technical operation of the system.

We show that the use of covariances helps to identify links that cannot be observed using variances alone. They also enable the importance of the role of interconnections in explaining volatility spillovers to be described. We propose the use of covariances in spillover measures to avoid underestimating strong links between non-interconnected markets. Identifying volatility spillovers is crucial to improving integration in NEM because market alignment increases liquidity and reduces the volatility of electricity prices.

Our analysis presents useful information for market participants and regulators. In the short-run, given market structural characteristics, we show how the NEM reacts to different events such as plant closures, deployment of intermittent RES generation, days with extreme weather conditions, and outages. Hence, market participants might optimize their short- or long-term investment strategies in light of these results.

Regarding long-term planning by regulators, the Department of Industry, Science, Energy and Resources of the Australian Government indicates that Australia could be powered by renewable energy by 2030 in an optimistic scenario (Australian Government, 2000). The roadmap to net-zero emissions even by 2050 implies decommissioning a large proportion of fossil-fuel generation. Our analysis shows that volatility spillovers could be larger if this process was unbalanced across states and appropriate investments in interconnections are not made. In this context, Project Energy Connect (Australian Energy Regulator, AER, 2020) is a role model.

CRediT authorship contribution statement

Evelyn Chanatásig-Niza: Conceptualization, Methodology, Software, Data curation, Writing – original draft, Writing – review & editing. **Aitor Ciarreta:** Conceptualization, Methodology, Data curation, Writing – original draft, Writing – review & editing. **Ainhoa Zarraga:** Conceptualization, Methodology, Data curation, Writing – original draft, Writing – review & editing.

Acknowledgments

The authors would like to thank two anonymous reviewers for valuable comments and suggestions that helped to improve the paper. Financial support from Ministerio de Ciencia e Innovación under research grant PID2019-108718GB-I00 and from Dpto. de Educación del Gobierno Vasco under research grant IT1336-19 is acknowledged. Evelyn Chanatásig thanks the University of the Basque Country, UPV/EHU, for financial aid under the trainee researcher program for Ph.D. students from Latin America. Open access funding provided by the University of the Basque Country.

Appendix A. Interconnectors in the Australian NEM

See Table A.1.

Table A.1
Interconnector Capacity in the NEM.

From	To	Nominal capacity
Terranora Interconnector		
NSW	Queensland	107 MW
Queensland	NSW	210 MW
QN Interconnector		
NSW	Queensland	300 to 600 MW
Queensland	NSW	1078 MW
VIC1-NSW1 Interconnector		
Victoria	NSW	700 to 1600 MW
NSW	Victoria	400 to 1350 MW
Basslink Interconnector		
Tasmania	Victoria	594 MW
Victoria	Tasmania	478 MW
Heywood Interconnector		
Victoria	South Australia	600 MW
South Australia	Victoria	500 MW
Murraylink Interconnector		
Victoria	South Australia	220 MW
South Australia	Victoria	200 MW

The table contains information about the nominal capacity of the transmission lines that connect the various NEM regions (interconnectors).

Appendix B. Cross-border electricity exchange balance for the sample period

See Fig. B.1.

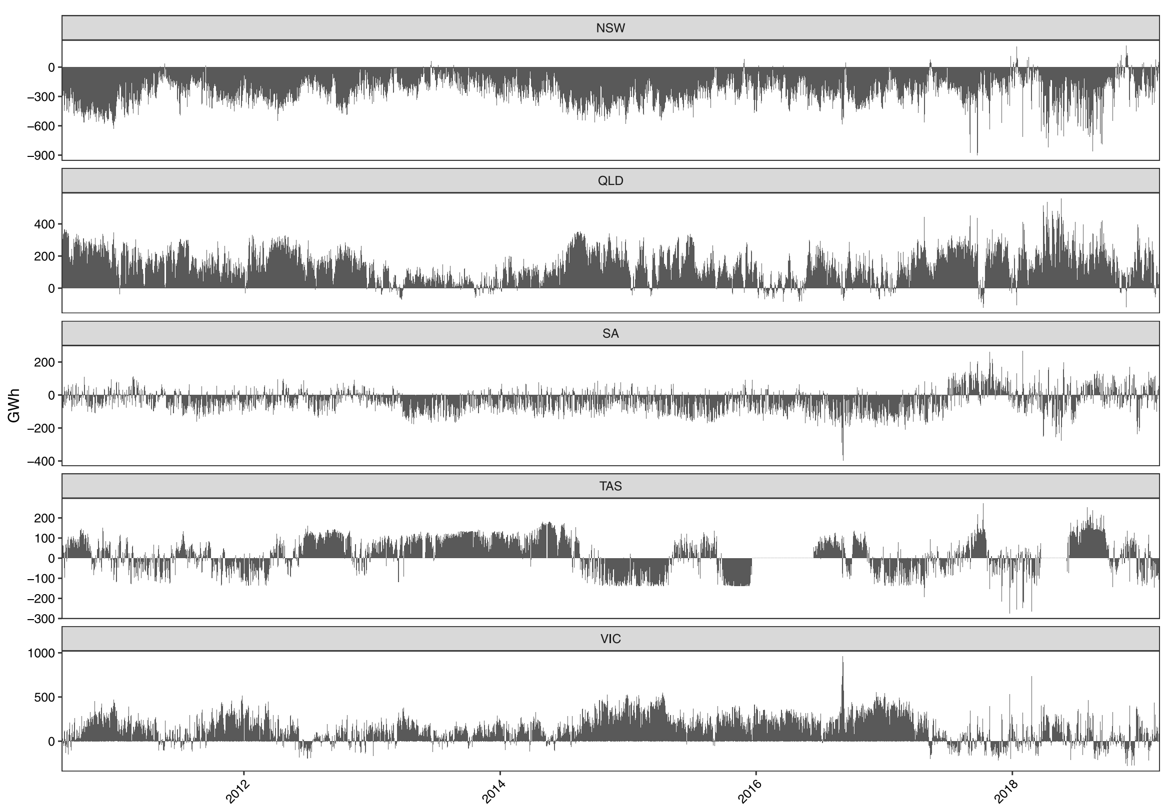

Fig. B.1. Cross-border exchange balance per state.
Note: Negative (positive) values indicate a net importing (exporting) position of the state.

Appendix C. Major events in the NEM

See Table C.1.

Table C.1
Events in the NEM reported by the AER.
Source: State of Energy Market reports provided by AER.

Date	Region	Causes identified by the AER
Coal plant closures		
3 July 2012	NSW	Munmorah Power Station was retired by Delta Electricity in 2012. Its capacity was 600 MW. First plant in NSW to shutdown under CPM.
1 December 2012	QLD	Collinsville Power Station closed in 2012 with the loss of 180 MW. First plant in QLD to shutdown under CPM.
30 August 2014	VIC	Morwell Power Station closed in 2014 after 56 years operating. Its capacity was 195 MW.
31 October 2014	NSW	Redbank Power Station, located in the Hunter Valley, had a capacity of 151 MW.
1 November 2014	NSW	Wallerawang was a thermal coal power station located near the town of the same name. In 2014 EnergyAustralia announced that the plant would close due to lack of access to competitively priced coal, high operating costs and a decrease in energy demand. Capacity at Wallerawang was 1000 MW.
8 May 2016	SA	Playford B Power Station was located at Port Paterson. It was coal powered and had a capacity of 240 MW.
9 May 2016	SA	Northern Power Station was located at Port Paterson. It was coal powered and had a capacity of 540 MW.
1 April 2017	VIC	The Hazelwood power station was a 1600 MW generator located in the La Trobe Valley in Victoria. The plant accounted for around 15% of installed capacity and supplied 20% of the state's electricity.
Days with high demand		
31 January, 1 and 2 February 2011	VIC, NSW, QLD	High temperatures led to demand reaching its highest level in Victoria, and New South Wales for the summer. The events affected neighboring regions such as Queensland.
29 November 2012	VIC, SA	Prices were driven by higher than expected temperatures causing electricity demand in Victoria and South Australia to significantly exceed forecasts.
15 December 2013	SA	The hottest December day since 1931.
19 and 20 December 2013	NSW, SA	High demand due to extreme heat was a key contributor. A plant outage, a lower than forecast contribution from wind and constraints limiting interconnector import flows also contributed to tight supply conditions.
15 January 2014	SA, VIC	Prices were lower than forecast during one of south east Australia's most intense heatwaves on record. Spare generation capacity was extremely tight on the day.
17 December 2014, and 15 and 18 January 2015	QLD	Events occurred on days of high temperatures and high demand, and network constraints affected supply in some instances.
5 March 2015	QLD, NSW	A heatwave in Brisbane caused maximum demand, setting a new Queensland record on 5 March, and long term network constraints limited electricity imports from NSW.
18 January 2017	QLD	Queensland recorded persistently high prices over January and February 2017. On this day, the events were intensified by peak demand, rising to record levels.
8 February 2017	NEM	A heatwave, when 42 degree temperatures fueled above forecast demand at a time when wind generation was below forecast.
19 January 2018	VIC, SA	High temperatures all around Australia but more intense in VIC and SA, coupled with a Victoria generator outage and bushfire risks.
24 and 25 January 2019	VIC, SA	2019. Record temperatures in the whole country, particularly high in VIC and SA, caused a surge in demand. This surge coincided with unexpected equipment failures.
Technical issues		
3 February 2011	QLD	Cyclone Yasi affected North Queensland, causing more than 170,000 homes to lose electricity.
21 December 2015	TAS	A fault occurred on the Basslink Interconnector running between Victoria and Tasmania, separating Tasmania from the National Electricity Market. The link was restored on 13 June 2016.
28 September 2016	SA	Extreme weather and infrastructure failures caused the entire state of South Australia to be blacked out for several hours.
1 December 2016	SA	The market experienced disruption soon after midnight, when a fault on one of the Heywood interconnector's two lines occurred during maintenance on the other line. SA was isolated from the NEM.

Appendix D. Directional spillovers for covariances

See Figs. D.1 and D.2.

Fig. D.1. Time-varying spillovers based on MHAR-ReCov (Covariances).
Note: Panel A shows the contribution of variances (dark orange) and covariances (light orange) to the directional spillovers. Panel B shows the net directional spillovers.

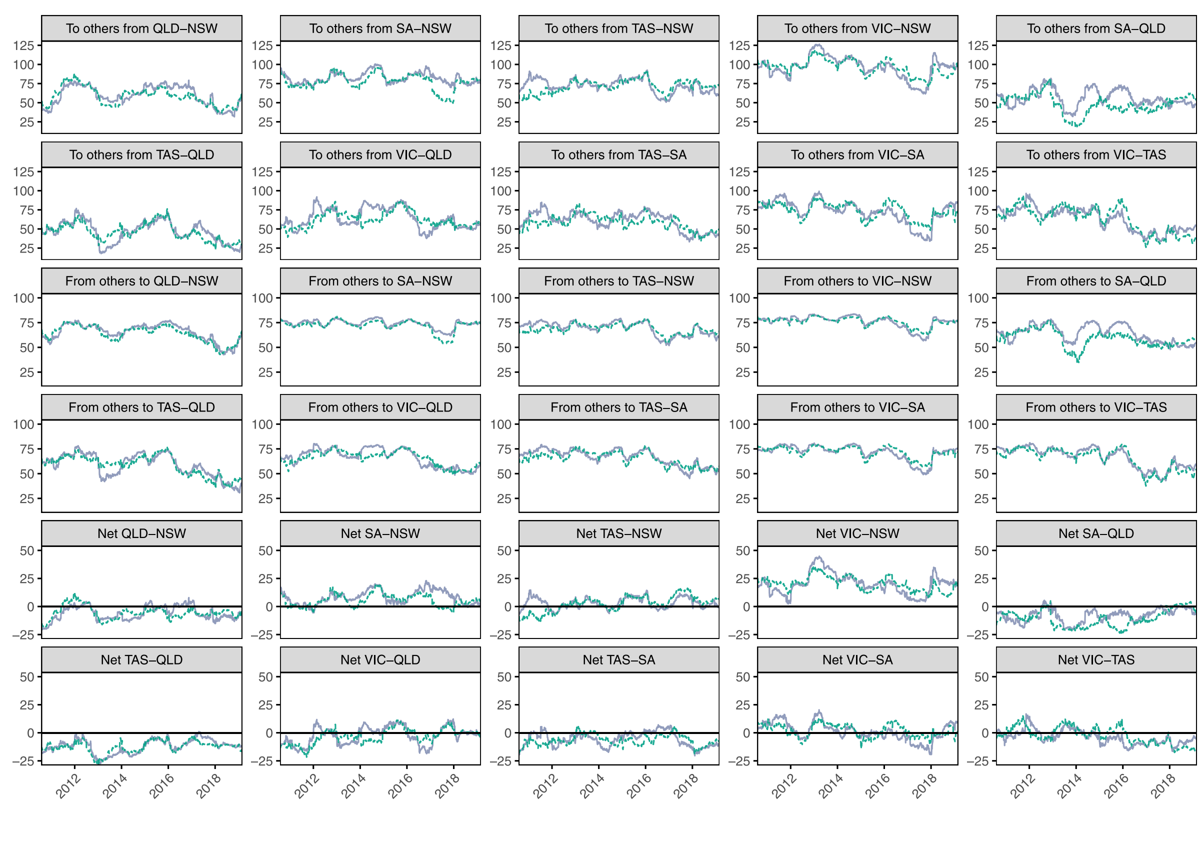

Fig. D.2. Time-varying spillovers based on MHAR-ReCov$^+$ and MHAR-ReCov$^-$ (Covariances).

Appendix E. Supplementary data

Supplementary material related to this article can be found online at https://doi.org/10.1016/j.eneco.2022.106076.

References

Andersen, T.G., Bollerslev, T., Diebold, F.X., Ebens, H., 2001. The distribution of realized stock return volatility. J. Financ. Econ. 61 (1), 43–76.

Apergis, N., Baruník, J., Lau, M.C.K., 2017. Good volatility, bad volatility: What drives the asymmetric connectedness of Australian electricity markets? Energy Econ. 66, 108–115.

Apergis, N., Gozgor, G., Lau, C.K.M., Wang, S., 2019. Decoding the Australian electricity market: New evidence from three-regime hidden semi-Markov model. Energy Econ. 78, 129–142.

Audrino, F., Knaus, S.D., 2016. Lassoing the HAR model: A model selection perspective on realized volatility dynamics. Econometric Rev. 35 (8–10), 1485–1521.

Australian Energy Market Commission, AEMC, 2020. National electricity rules Version 161. Australian Energy Market Commission.

Australian Energy Market Operator, AEMO, 2020. Fact sheet: The national electricity market.

Australian Energy Regulator, AER, 2010. State of the Energy Market 2010. Australian Energy Regulator.

Australian Energy Regulator, AER, 2012. State of the Energy Market 2012. Australian Energy Regulator.

Australian Energy Regulator, AER, 2013. State of the Energy Market 2013. Australian Energy Regulator.

Australian Energy Regulator, AER, 2014. State of the Energy Market 2014. Australian Energy Regulator.

Australian Energy Regulator, AER, 2017. State of the Energy Market 2017. Australian Energy Regulator.

Australian Energy Regulator, AER, 2020. State of the Energy Market 2020. Australian Energy Regulator.

Australian Government, 2000. Renewable Energy (Electricity) Act 2000. Clean Energy Regulator.

Barndorff-Nielsen, O., Kinnebrock, S., Shephard, N., 2010. Volatility and Time Series Econometrics: Essays in Honor of Robert F. Engle. Chapter: Measuring Downside Risk-Realised Semivariance. Oxford University Press.

Baruník, J., Kocenda, E., Vácha, L., 2015. Volatility spillovers across petroleum markets. Energy J. 36 (3), 309–329.

Bollerslev, T., 2021. Realized semi(co)variation: Signs that all volatilities are not created equal, Economic Research Initiatives at Duke (ERID) Working Paper 306.

Bollerslev, T., Li, J., Patton, A.J., Quaedvlieg, R., 2020. Realized semicovariances. Econometrica 88 (4), 1515–1551.

Brinsmead, T.S., Hayward, J., Graham, P., 2014. Australian electricity market analysis report to 2020 and 2030. CSIRO Technical Report No. EP141067.

Bunn, D.W., Gianfreda, A., 2010. Integration and shock transmissions across European electricity forward markets. Energy Econ. 32 (2), 278–291.

Chan, K.F., Gray, P., van Campen, B., 2008. A new approach to characterizing and forecasting electricity price volatility. Int. J. Forecast. 24 (4), 728–743.

Ciarreta, A., Zarraga, A., 2015. Analysis of mean and volatility price transmissions in the MIBEL and EPEX electricity spot markets. Energy J. 36 (4), 41–60.

Ciarreta, A., Zarraga, A., 2016. Modeling realized volatility on the spanish intra-day electricity market. Energy Econ. 58, 152–163.

Corsi, F., 2009. A simple approximate long-memory model of realized volatility. J. Financ. Econom. 7 (2), 174–196.

Cramton, P., 2017. Electricity market design. Oxf. Rev. Econ. Policy 33, 589–612.

Diebold, F.X., Yilmaz, K., 2009. Measuring financial asset return and volatility spillovers, with application to global equity markets. Econ. J. 119 (534), 158–171.

Diebold, F.X., Yilmaz, K., 2012. Better to give than to receive: Predictive directional measurement of volatility spillovers. Int. J. Forecast. 28 (1), 57–66.

Diebold, F.X., Yilmaz, K., 2014. On the network topology of variance decompositions: Measuring the connectedness of financial firms. J. Econometrics 182 (1), 119–134.

Do, H.X., Nepal, R., Jamasb, T., 2020. Electricity market integration, decarbonisation and security of supply: Dynamic volatility connectedness in the irish and great britain markets. Energy Econ. 92, 104947.

Fengler, M.R., Gisler, K.I., 2015. A variance spillover analysis without covariances: What do we miss? J. Int. Money Finance 51, 174–195.

Han, L., Kordzakhia, N., Trück, S., 2020. Volatility spillovers in Australian electricity markets. Energy Econ. 90, 104782.

Higgs, H., 2009. Modelling price and volatility inter-relationships in the Australian wholesale spot electricity markets. Energy Econ. 31, 748–756.

Ignatieva, K., Trück, S., 2016. Modeling spot price dependence in Australian electricity markets with applications to risk management. Comput. Oper. Res. 66, 415–433.

International Energy Agency, IEA, 2020. OECD – Coal statistics.

Knittel, C.R., Roberts, M.R., 2005. An empirical examination of restructured electricity prices. Energy Econ. 27, 791–817.

Koop, G., Pesaran, M., Potter, S.M., 1996. Impulse response analysis in nonlinear multivariate models. J. Econometrics 74 (1), 119–147.

Lindström, E., Regland, F., 2012. Modeling extreme dependence between European electricity markets. Energy Econ. 34 (4), 899–904.

Lütkepohl, H., 2000. Bootstrapping Impulse Responses in VAR Analyses. Technical report, Humboldt University of Berlin, Interdisciplinary Research Project 373.

Park, H., Mjelde, J.W., Bessler, D.A., 2006. Price dynamics among US electricity spot markets. Energy Econ. 28 (1), 81–101.

Pesaran, H.H., Shin, Y., 1998. Generalized impulse response analysis in linear multivariate models. Econom. Lett. 58 (1), 17–29.

Tibshirani, R., 1996. Regression shrinkage and selection via the lasso. J. R. Stat. Soc. Ser. B Stat. Methodol. 58 (1), 267–288.

Trancoso, R., Syktus, J., Toombs, N., Ahrens, D., Wong, K.K.-H., Pozza, R.D., 2020. Heatwaves intensification in Australia: A consistent trajectory across past, present and future. Sci. Total Environ. 742, 140521.

Uniejewski, B., Weron, R., Ziel, F., 2017. Variance stabilizing transformations for electricity spot price forecasting. IEEE Trans. Power Syst. 33 (2), 2219–2229.

Wilson, R., 2002. Architecture of power markets. Econometrica 70 (4), 1299–1340.

Worthington, A., Kay-Spratley, A., Higgs, H., 2005. Transmission of prices and price volatility in Australian electricity spot markets: A multivariate GARCH analysis. Energy Econ. 27, 337–350.

Yan, G., Trück, S., 2020. A dynamic network analysis of spot electricity prices in the Australian national electricity market. Energy Econ. 92, 104972.